

NACA RM L58E14

OTS PRICE

~~SECRET~~ 51-64808

514  
Copy  
RM L58E14

X62-64808

19p.

**NACA**

**63 18043**  
*Code-1*

# RESEARCH MEMORANDUM

AN INVESTIGATION OF THE EFFECT OF TARGET TEMPERATURE  
ON PROJECTILE PENETRATION AND CRATERING

By William H. Kinard and C. H. Lambert, Jr.

Langley Aeronautical Laboratory  
Langley Field, Va.

*1.60 per  
2.80 per*

XEROX \$  
MICROFILM \$

~~SECRET~~

**NATIONAL ADVISORY COMMITTEE  
FOR AERONAUTICS**

**WASHINGTON**

July 28, 1958

~~SECRET~~

[REDACTED]

## NATIONAL ADVISORY COMMITTEE FOR AERONAUTICS

## RESEARCH MEMORANDUM

AN INVESTIGATION OF THE EFFECT OF TARGET TEMPERATURE  
ON PROJECTILE PENETRATION AND CRATERING\*

By William H. Kinard and C. H. Lambert, Jr.

## SUMMARY

18043

Results of steel projectiles fired into copper targets at velocities from 5,000 to 11,500 feet per second indicate that as the target temperature is increased the crater size also increases. Projectiles impacting targets heated to 900° F produced craters having as much as twice the volume of craters produced by projectiles of the same type impacting targets having a temperature of 80° F. It appears that the decreasing of the speed of sound in the target material as it is heated can be used as a parameter to predict the amount of increased cratering to be expected when targets are heated.

Twenty-two caliber steel cylinders having length-to-diameter ratios of  $\frac{1}{2}$  and 1 and steel spheres having a diameter of  $\frac{1}{16}$  inch were used as the projectiles. It was noted from the data obtained that the values of the penetration produced by the impacting cylinders divided by the length of the cylinders are very near the values of the penetration produced by the spheres divided by the length of an equivalent cylinder having the same mass and moment of inertia about the longitudinal axis as the spherical projectiles when all other factors are held identical.

## INTRODUCTION

The vulnerability of space vehicles, satellites, and long-range missiles to damage by collision with meteors and other small particles has been the subject of various investigations. (See, for example, ref. 1.) Since it is realized that hypersonic vehicles may reach relatively high skin temperatures at some portion of their trajectory, it is of interest to see what effect the skin temperature has on the penetration and on the crater formed by an impacting object. This investigation was conducted in order to study the behavior of copper at various

---

\*Title, Unclassified.  
[REDACTED]

temperatures when impacted by steel projectiles traveling at velocities up to 11,500 feet per second.


### SYMBOLS

C	speed of sound in target material, $\sqrt{\frac{E}{\rho_T}}$ , ft/sec
d	projectile diameter, in.
E	Young's modulus
K	a constant
L	length of projectile, in.
$L^1$	length of fictitious cylinder having same M and I as sphere ( $L^1 = 1.2 \times$ sphere diameter), in.
M	mass of projectile, slugs
I	moment of inertia of projectile about longitudinal axis, lb-in. <sup>2</sup>
P	penetration, in.
V	projectile velocity, ft/sec
$\rho$	density, slug-ft <sup>3</sup>
Subscripts:	
P	projectile
T	target

### APPARATUS AND TEST TECHNIQUE

#### Description of Guns and Projectiles


Photographs of the two guns used to accelerate the cylinders and spheres in this investigation are shown in figures 1 and 2. Figure 1



shows a standard 220 Swift rifle that was used to propel 0.22-inch-diameter steel cylinders having length-to-diameter ratios of  $1/2$  to a velocity of 5,950 feet per second and steel cylinders of the same diameter having length-to-diameter ratios of 1 to a velocity of 5,000 feet per second. The velocities of the cylinders were measured by allowing the cylinders to break two painted circuits, shown in figure 1, and recording the time interval between the breaking of each circuit on a Hewlett-Packard precision electronic-counter with a time interval unit. The cylinders were constructed from cold-rolled SAE 1020 steel.

Figure 2 shows the helium gun which was used to shoot the  $\frac{1}{16}$ -inch-diameter steel spheres to a velocity of 11,500 feet per second. The helium gun consists of a 20-millimeter pump tube and a .22-caliber launch tube which is connected to a vacuum chamber. For the firings in this investigation a helium pressure of 900 lb/sq in. and a powder charge of 450 grains of Hercules Unique rifle powder were used in the pump tube. The helium in the pump tube is compressed by a shock wave formed by the burning powder charge and provides the force to launch the projectile. The launching tube and vacuum chamber were evacuated to a pressure of 1 millimeter of mercury. Two 0.001-inch-thick sheets of aluminum foil were placed in the vacuum tank and were visible from the outside through the tank side windows. As the steel sphere impacted each foil sheet, a blip of light was generated. By recording these blips on a high-speed drum camera with the film moving in a plane perpendicular to the flight path of the sphere, the velocity of the sphere was determined. One steel sphere was recovered after impacting the aluminum foil by allowing it to penetrate into Styrofoam. The fact that no damage could be observed on the sphere indicates that the foil did not harm it. The steel spheres were mounted on the front of nylon sabots in order to facilitate shooting them in the .22-caliber launch tube. Several inches down range from the muzzle of the launch tube the sabot was deflected from the flight path of the sphere by a steel plate which protruded into the projected cross section of the launch-tube bore just far enough to be struck by the sabot but not far enough to be hit by the smaller sphere; therefore, the impact of the sphere alone could be studied.

The velocities of projectiles fired from the 220 Swift rifle presented herein have been corrected for aerodynamic drag over the distance from the target to a point midway between the velocity-measuring grids. This correction was less than 2 percent of the measured velocities in all cases. The quoted velocities of all tests presented herein are believed to be accurate to within  $\pm 1$  percent.





### Description of Targets


All targets used in this investigation were made from commercially pure copper bar stock. The targets used with the 220 Swift rifle were 2 inches in diameter and 2 inches thick, whereas larger 4-inch-diameter targets had to be used with the helium gun in order to insure their being hit, since deflecting the sabot caused the spheres to deviate slightly from their original flight path.

The targets impacted at elevated temperatures were heated by a propane gas burner to a temperature above the temperature desired for the impact and then placed in the target holder and allowed to cool to the correct temperature before the firing. Temperatures of the targets were measured by thermocouples imbedded in the back of the targets and recorded on a Honeywell Electronik strip chart recorder. Targets used with the helium gun had to be heated 300° to 400° F above the intended temperature in order to allow sufficient time to place them in the vacuum chamber, seal the end, evacuate the chamber to the correct pressure, and prepare to fire the gun before the target cooled to the temperature intended.

### RESULTS AND DISCUSSION

Figures 3 and 4 show photographs of the copper targets impacted in this investigation. Figures 5 and 6 show graphs illustrating the effect of the temperature of the copper targets at the time of impact on the crater diameter, depth of penetration, and crater volume.

It can be seen in figures 5 and 6 that in targets heated to 900° F the diameter of the crater formed increased about 15 to 25 percent, the depth of penetration increased about 30 to 40 percent, and the volume increased about 75 to 175 percent over those of targets at 80° F impacted by the same type of projectile at the same velocity. The 900° F temperature was chosen as a point of comparison because it is the highest temperature at which all types of projectiles can be compared. The percent increase in volume due to the increase in target temperature was greater for cylinders than for spheres. Reference 1 indicates that the penetration of a high-velocity shot may be a function of the ratio of the speed of sound in the target material and the velocity of the impacting projectile. In the study reported in reference 2 it was found that the penetration also apparently is some function of the ratio of the density of the target material to the density of the projectile and that the equation



$$\frac{P}{d} = 2.28 \left( \frac{\rho_P}{\rho_T} \right)^{0.69} \left( \frac{V}{C} \right)^{0.69} \quad (1)$$

is approximately the equation of the line faired through the data points of this reference.

In the investigation reported in reference 3 spheres of various materials were impacted into targets of the same material; thus, the ratio  $\left( \frac{\rho_P}{\rho_T} \right)$  was equal to 1. The data from this investigation followed the relationship

$$\frac{P}{d} = K_P \left( \frac{V}{C} \right) \quad (2)$$

where  $K_P$  depended upon the material used for the projectile and target. For copper targets and projectiles it was found that  $K_P = 2.44$ .

In the present investigation, the ratio  $\left( \frac{\rho_P}{\rho_T} \right)$  was not equal to 1; therefore, equation (2) was modified to include the density ratio, as was done in equation (1), and the resulting equation

$$\frac{P}{d} = K \left( \frac{V}{C} \right) \left( \frac{\rho_P}{\rho_T} \right) \quad (3)$$

was obtained. The data obtained in this investigation appear to be described by equation (3) as shown by the graph of  $\frac{P}{L}$ , where  $L$  is the length of the cylinder or the diameter for the sphere, plotted against  $\left( \frac{\rho_P}{\rho_T} \right) \left( \frac{V}{C} \right)$  as shown in figure 7(a).

The value of  $K$  in equation (2) depends upon the material used for the projectile and target. In this investigation the target material and projectile material were held constant, and only the projectile shape was changed. Therefore,  $K$  in equation (3) is defined as

$$K = (K_t) (K_s) \quad (4)$$

where  $K_t$  is a factor describing the target material and  $K_s$  is a factor describing the projectile shape.  $K_s$  was arbitrarily chosen as 1 for a cylinder, and  $K_p$  can be found from figure 7 to be 2.85 for the copper targets used.  $K_s$  for the spherical projectiles was then established to be 0.765. In figure 7(b), values for the steel spheres have been plotted as equivalent values of cylinders of equal mass and moment of inertia around the longitudinal axis. It can be noted that the values for the spheres now fall in line with the values for the cylinders. In this investigation, this method seems to be a way in which all of the data can be correlated, and the  $K_s$  of equation (4) can be disregarded. It is felt that the deviation of the high-temperature points from the average curve of figure 7 may be caused by questionable values of Young's modulus for copper at the higher temperatures. The values of Young's modulus used in calculating  $C$  for the present tests were taken from reference 4.

Figure 8 shows a plot of  $\frac{P}{d}$  against  $\left(\frac{\rho_p}{\rho_T}\right)\left(\frac{V}{C}\right)$  for the data obtained by impacting the steel spheres into copper targets in this investigation and also the data from reference 3 obtained by impacting copper spheres into copper targets. The predicted penetration of equation (1) is also given for purposes of comparison. It can be noted that both sets of data agree very well with the plot of equation (3) which is also shown, but deviate from equation (1). It should be noted that penetration equations (1), (2), and (3) stem from a dimensional analysis of high-velocity impacts and are not obtained from a theoretical investigation of the physical phenomena. It is, therefore, probable that these equations can do no more than correlate data over some limited range of impact conditions.

#### CONCLUDING REMARKS

Results of impacts of .22-caliber steel cylinders having length-to-diameter ratios of  $\frac{1}{2}$  and 1 and of  $\frac{1}{16}$ -inch-diameter steel spheres into copper targets at velocities from 5,000 to 11,500 feet per second indicate that as the target temperature increases the crater size also increases. It appears that the decreasing of the speed of sound in the target material as it is heated can be used as a parameter to predict the amount of increased cratering that occurs when targets are heated.

Impacted copper targets which had been heated to 900° F showed craters about 15 to 25 percent larger in diameter than copper targets impacted at 80° F, while the depth of penetration increased about 30 to

[REDACTED]



40 percent. It appears that an equation containing the ratio of projectile velocity to speed of sound in the target material and the ratio of projectile density to target density can be used to predict the depth of penetration to be expected in high-velocity impacts.

Langley Aeronautical Laboratory,  
National Advisory Committee for Aeronautics,  
Langley Field, Va., April 21, 1958.

#### REFERENCES

1. Huth, J. H., Thompson, J. S., and Van Valkenburg, M. E.: Some New Data on High-Speed Impact Phenomena. Jour. Appl. Mech., vol. 24, no. 1, Mar. 1957, pp. 65-68.
2. Charters, A. C., and Locke, G. S., Jr.: A Preliminary Investigation of High-Speed Impact: The Penetration of Small Spheres into Thick Copper Targets. NACA RM A58B26, 1958.
3. Partridge, William S., VanFleet, Howard B., and Whited, Charles R.: An Investigation of Craters Formed by High-Velocity Pellets. Tech. Rep. No. OSR-9 (Contract No. AF 18(600)1217), Dept. Elec. Eng., Univ. of Utah, May 1957. (Available from ASTIA as AD No. 132364.)
4. Kattus, J. Robert, and Dotson, Clifford L.: Tensile, Fracture, and Short-Time Creep Properties of Aircraft-Structural Materials at Very High Temperatures After Rapid Heating. WADC Tech. Rep. 55-391, ASTIA Doc. No. AD 110560, U. S. Air Force, Dec. 1955.



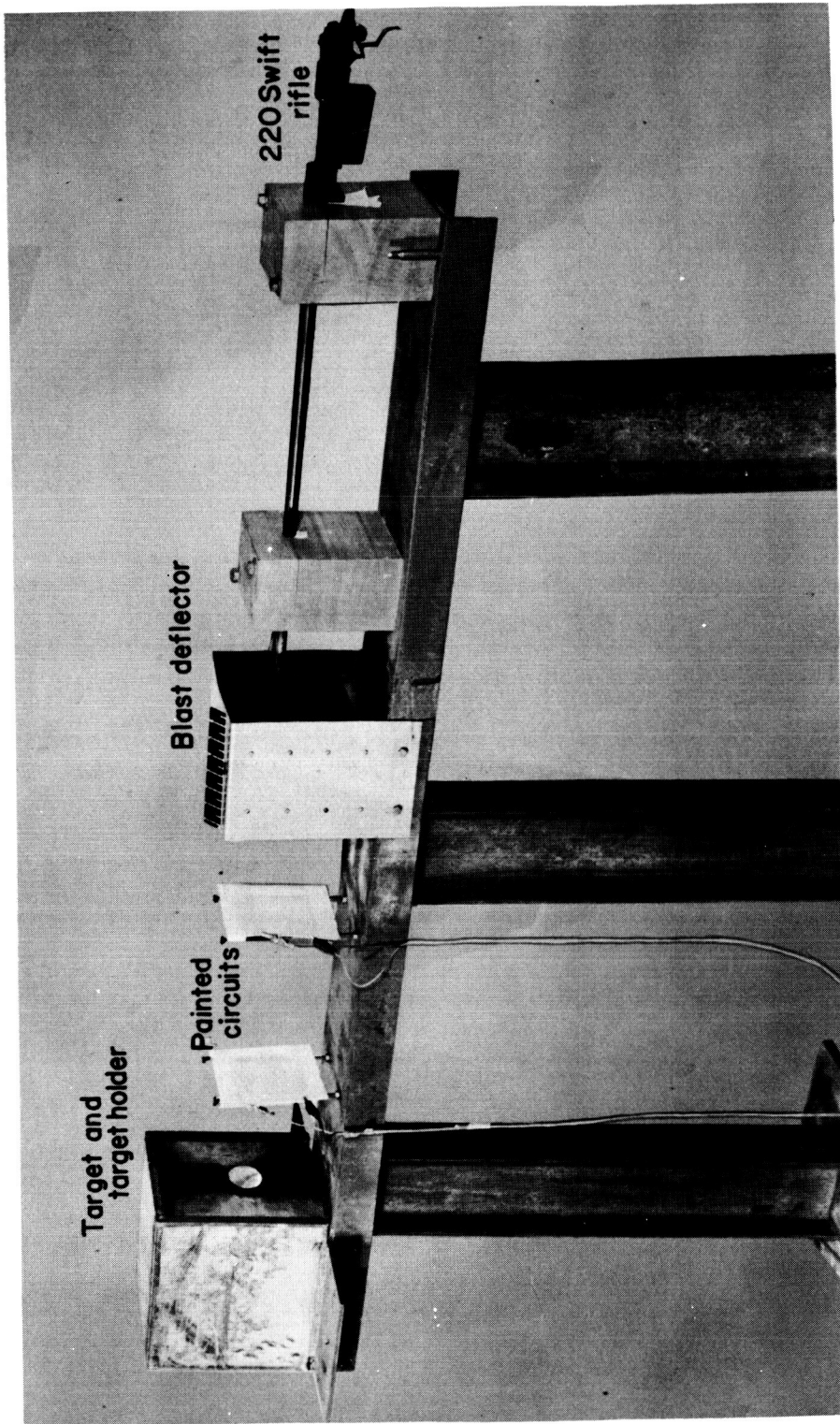


Figure 1.- General arrangement of 220 Swift rifle used in making impact studies. L-57-3298.1

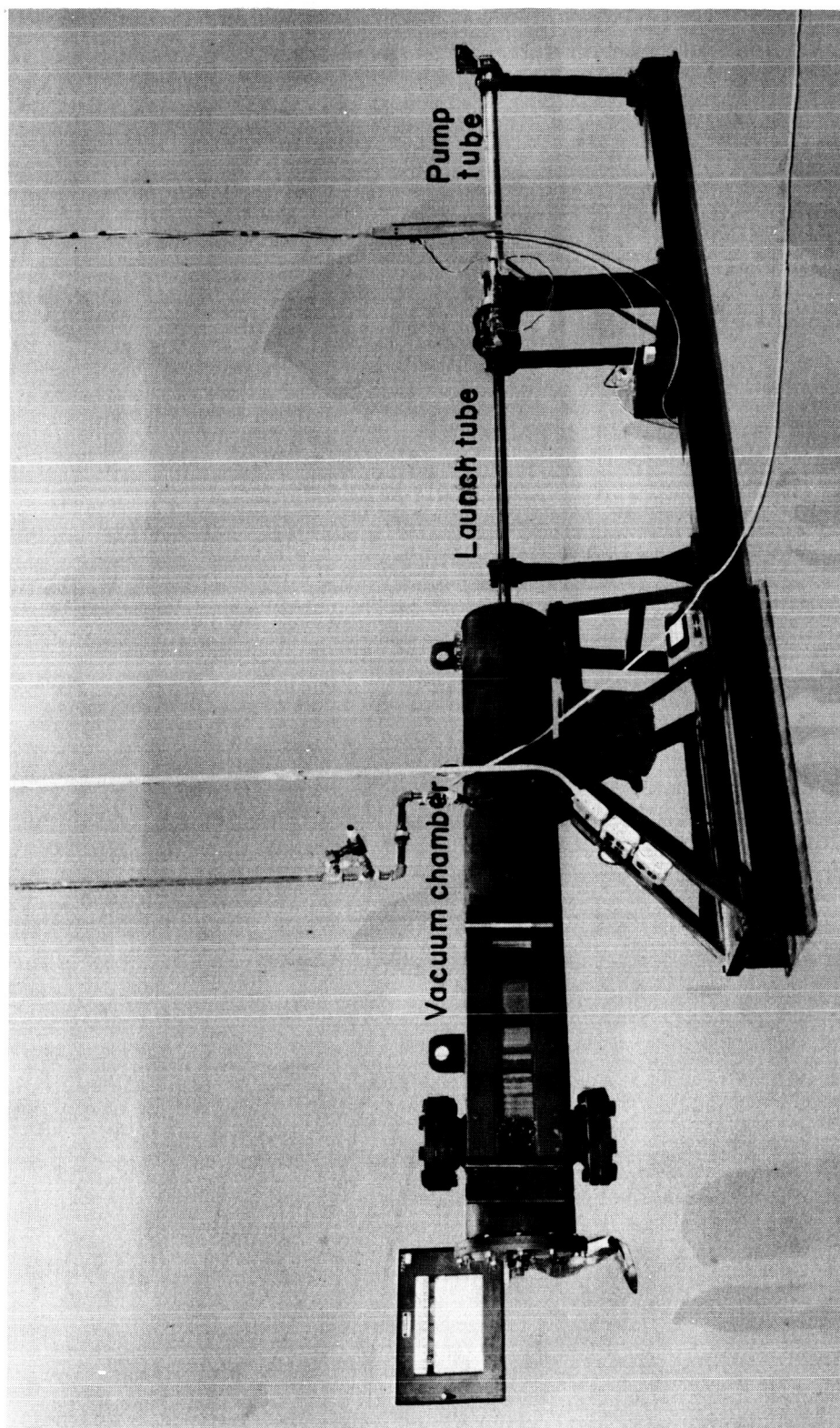

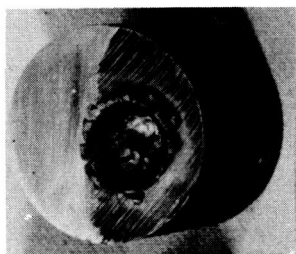
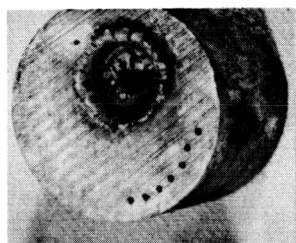


Figure 2.-- Helium-gun installation. L-57-4364.1

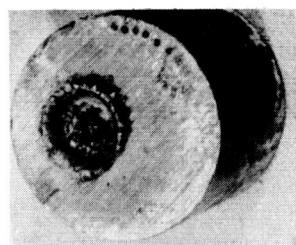
Scale: 0  Inches



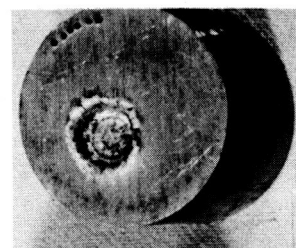
1450°F



1050°F

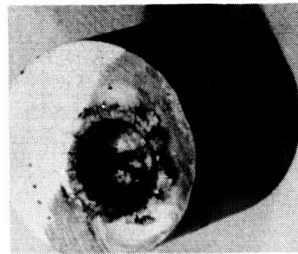


495°F

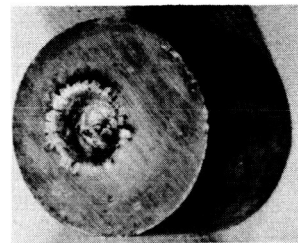


80°F

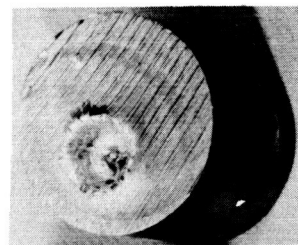
(a) .22-caliber steel cylinders.  $\frac{L}{d} = 1$ ; velocity = 5,000 ft/sec.



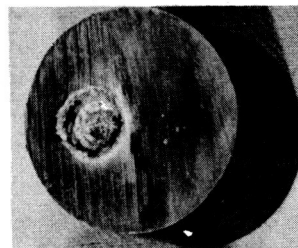
1425°F



1050°F



525°F

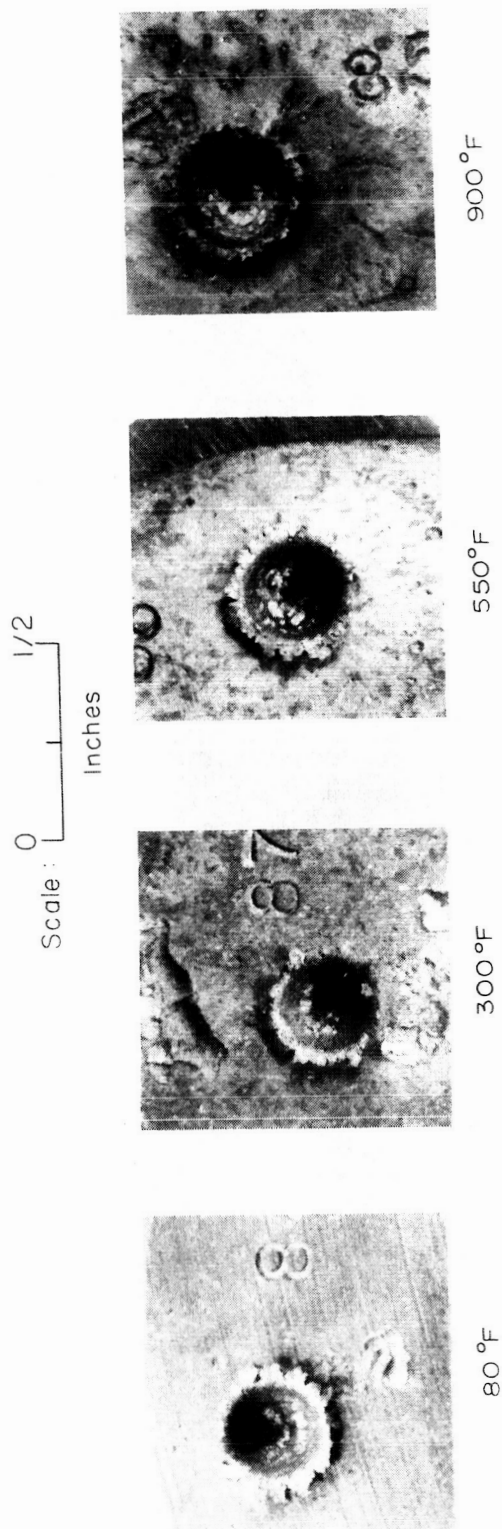


80°F

(b) .22-caliber steel cylinders.  $\frac{L}{d} = 0.5$ ; velocity = 5,950 ft/sec. L-58-1630

Figure 3.- Copper targets after being impacted by steel cylinders.



~~CONFIDENTIAL~~

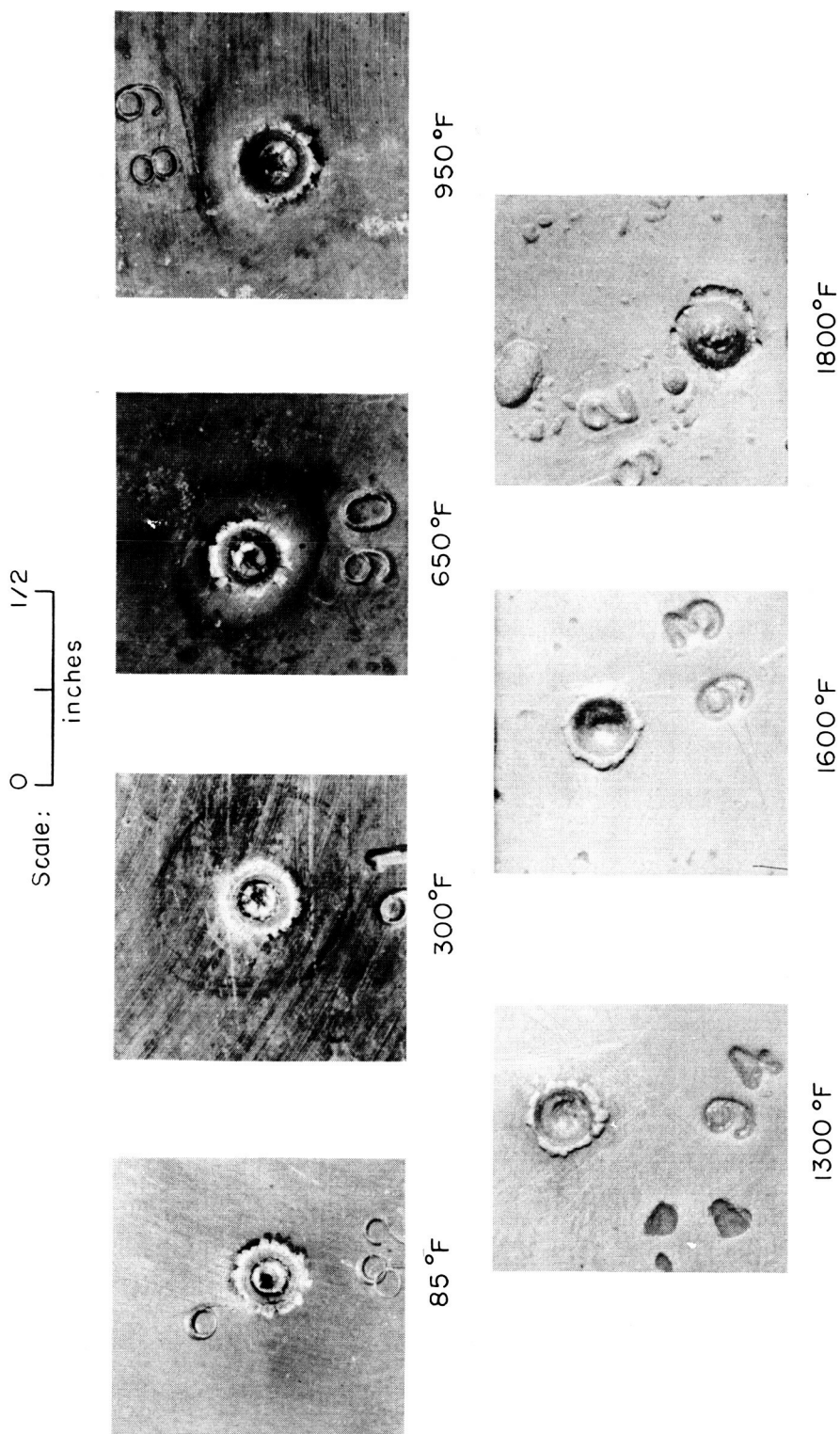
(a) Projectile velocity = 11,500 ft/sec. L-58-1631

Figure 4.- Copper targets after being impacted by  $\frac{1}{16}$ -inch steel spheres.

~~CONFIDENTIAL~~



03712 ~~XXXXXXXXXX~~ 03



(b) Projectile velocity = 6,400 ft/sec. L-58-1632

Figure 4.- Concluded.

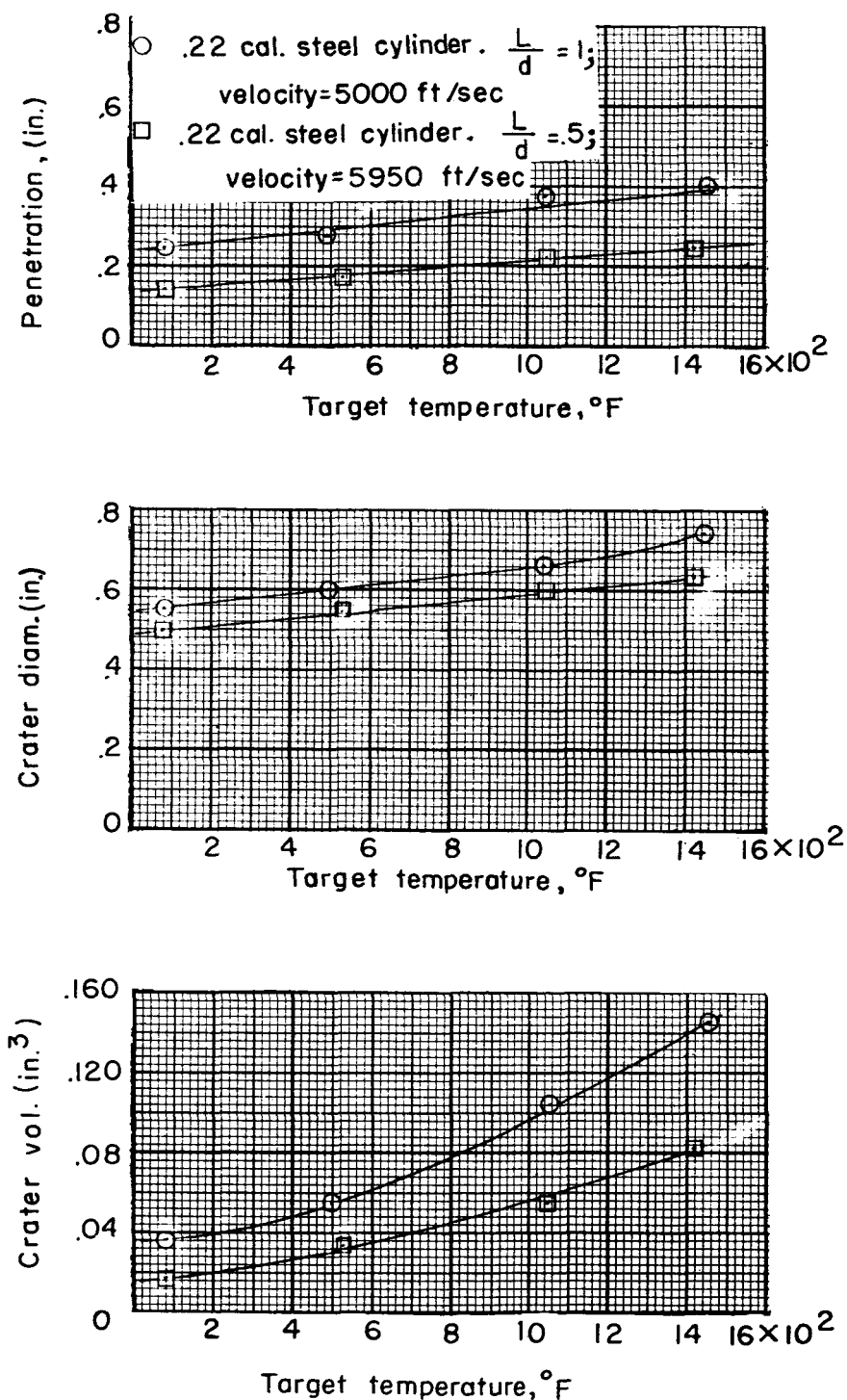
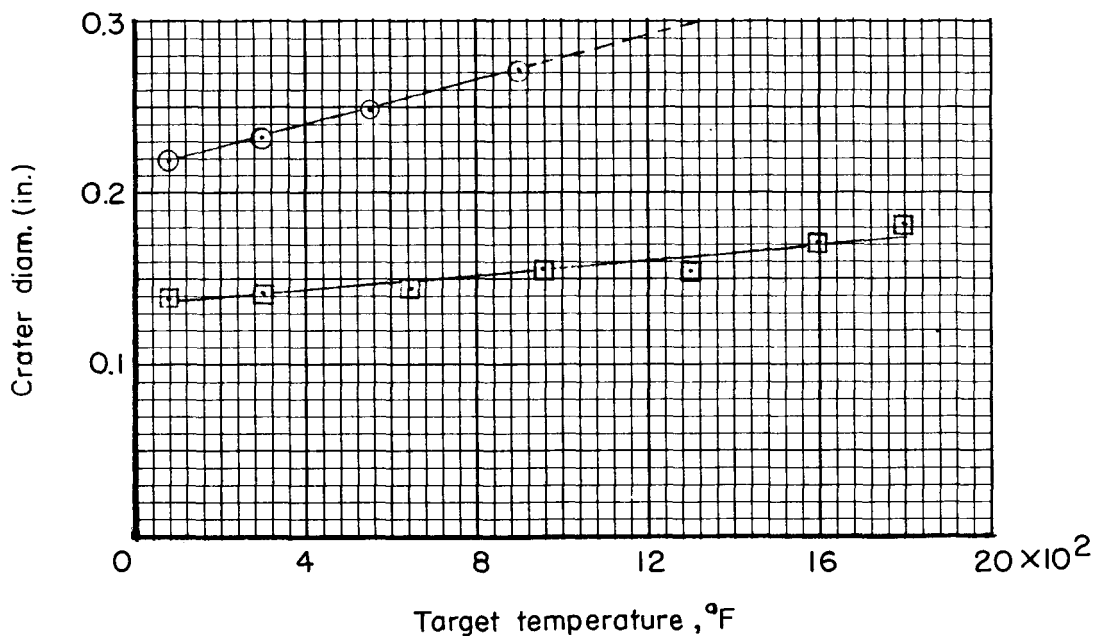
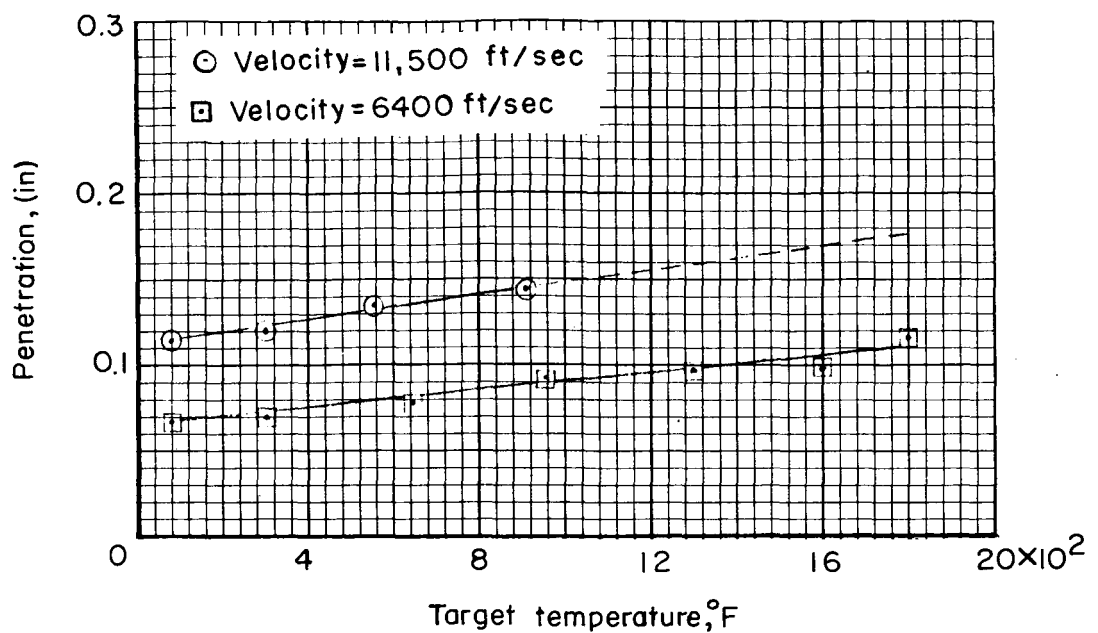
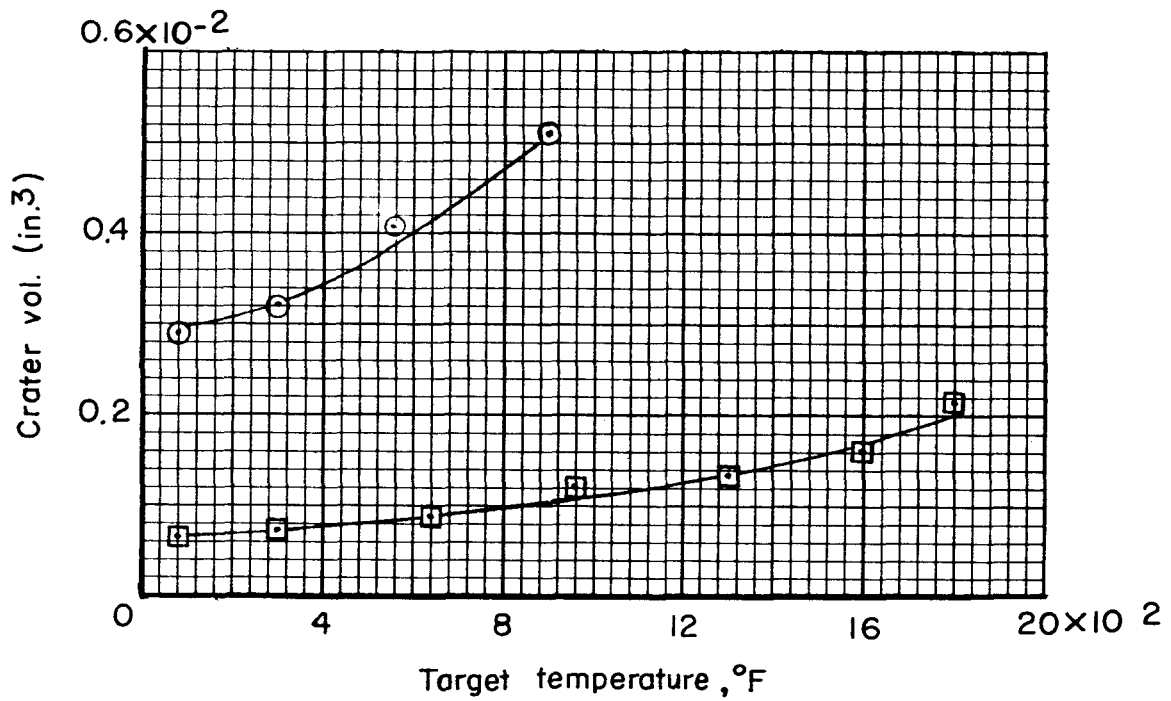


Figure 5.- Effect of target temperature on cratering by impacting cylinders.



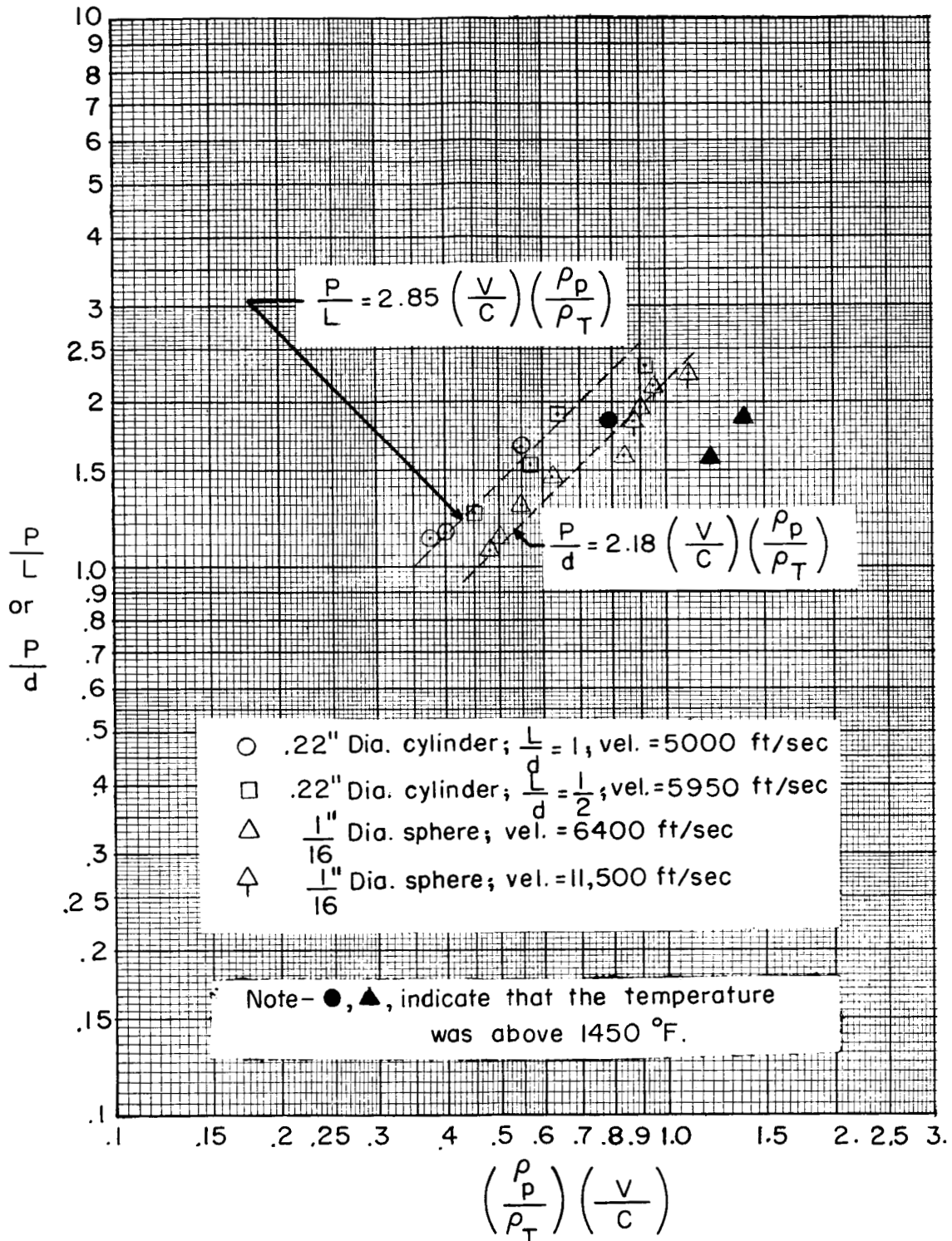
(a) Crater diameter and projectile penetration.

Figure 6.- Effect of target temperature on cratering by impacting spheres.



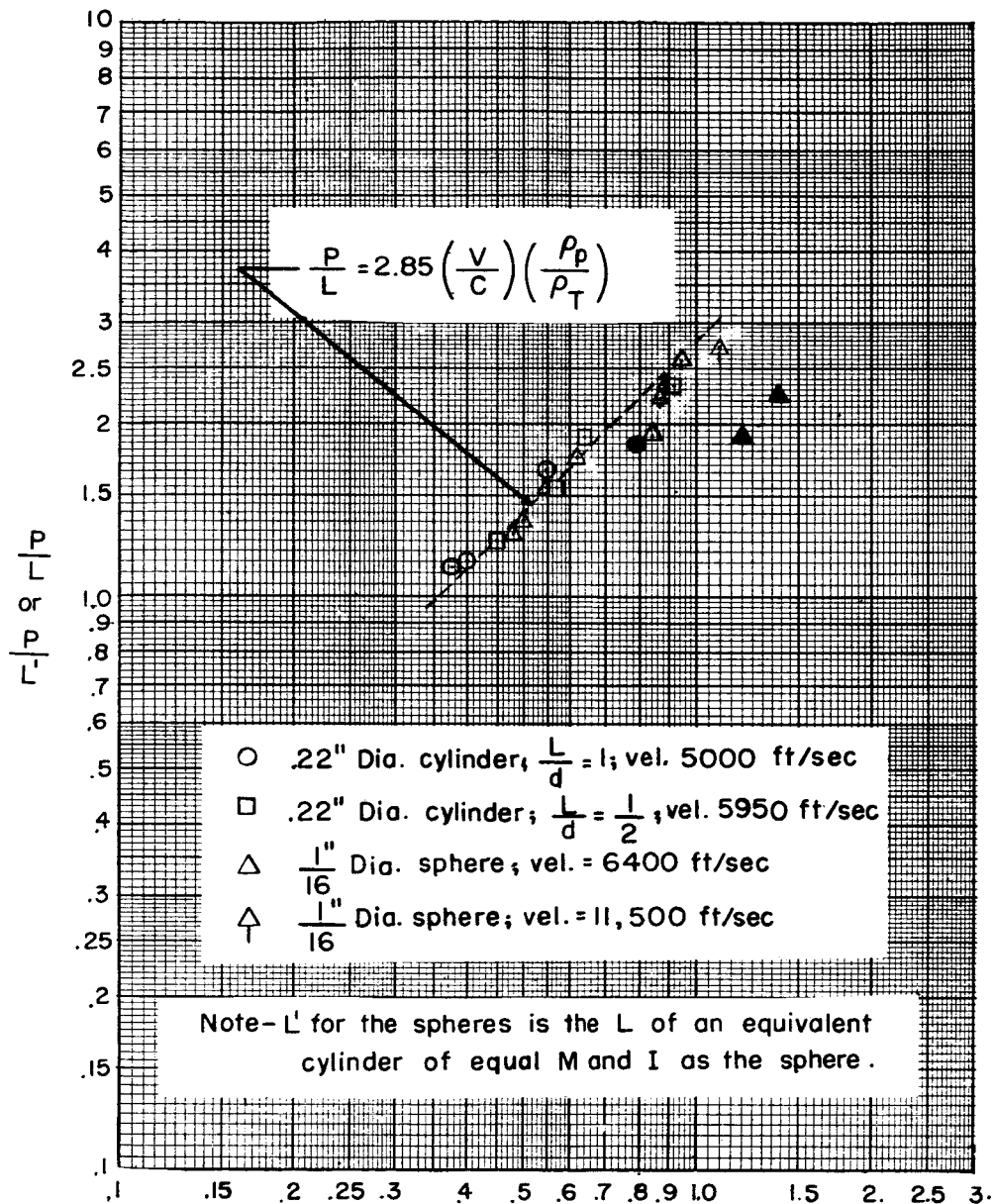
(b) Crater volume.

Figure 6.- Concluded.



(a) Target penetration divided by projectile length.

Figure 7.- Data obtained by impacting copper targets heated from 80° F to 1,800° F.



$$\left( \frac{\rho_p}{\rho_T} \right) \left( \frac{v}{c} \right)$$

(b) Target penetration divided by projectile length  $L$  (cylinders) or equivalent length  $L'$  (spheres).

Figure 7.- Concluded.

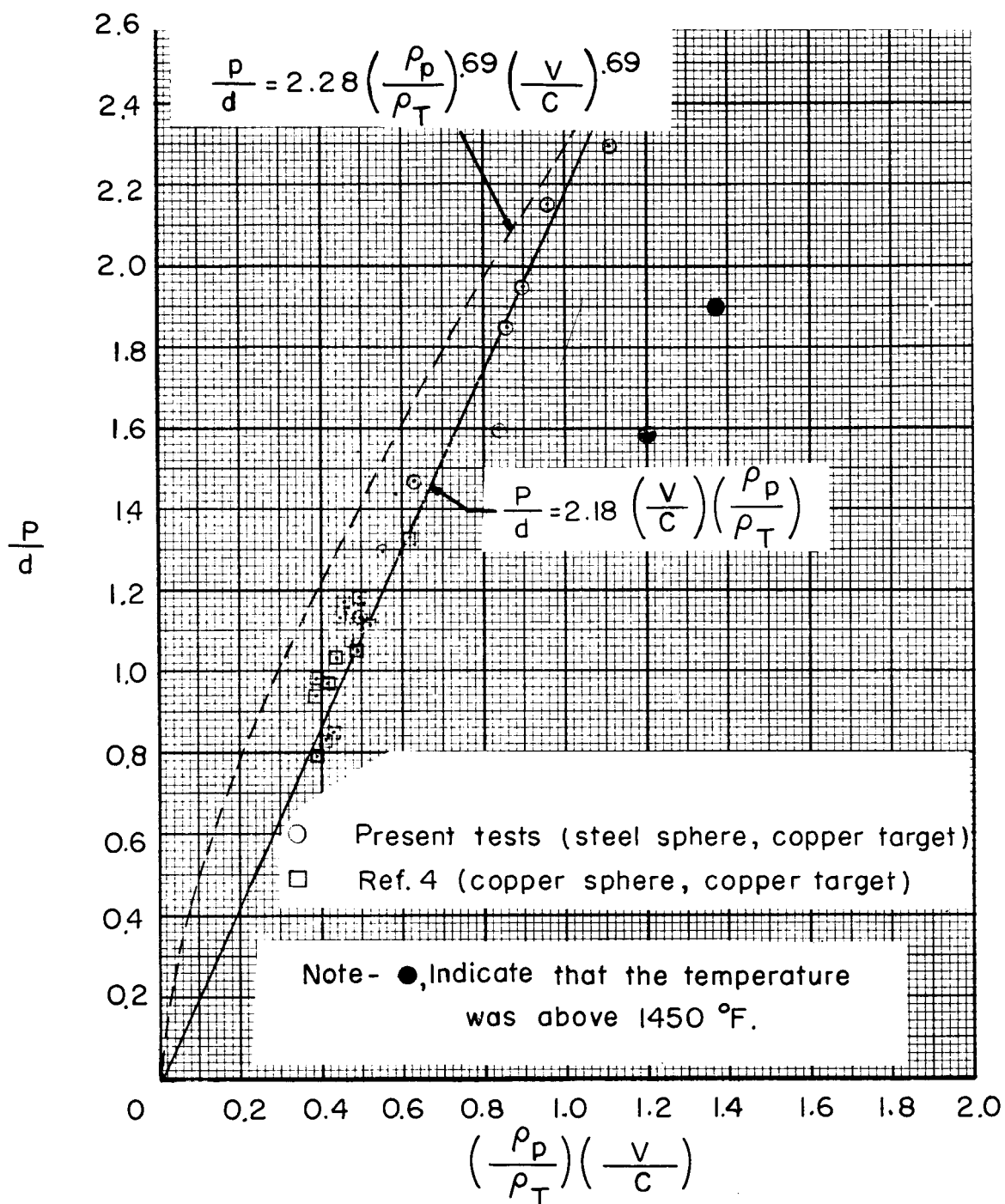


Figure 8.- Comparison of impact penetration data obtained in reference 4 and this investigation with predicted penetration of reference 3.